

---

*Received October 19, 2016; reviewed; accepted March 20, 2017*

## **Investigation on the particle size and shape of iron ore pellet feed using ball mill and HPGR grinding methods**

**Armin Abazarpoor, Mohammad Halali**

Materials Science & Engineering Department, Sharif University of Technology, Azadi Street,  
PO box 11365-11155, Tehran, Iran, Corresponding author: abazarpoor@mehr.sharif.edu (Armin Abazarpoor)

---

**Abstract:** An effect of a grinding method, that is ball mill and high pressure grinding rolls (HPGR), on the particle size, specific surface area and particle shape of an iron ore concentrate was studied. The particle size distribution was meticulously examined by sieve, laser and image analyses. To measure the specific surface area of particles, Brunauer-Emmett-Teller (BET) and Blaine methods were used. It was found that for samples having equal Blaine specific surface areas numbers, the amount of fine particles produced in HPGR was higher than that produced in a ball mill. A higher surface area was observed from HPGR treatment in comparison to ball mill grinding, provided by a higher porosity, cracks, roughness and new surfaces. A shape factor of particles was determined using the circularity, roughness, and aspect ratio. It was also observed that HPGR produced particles that were more elongated, less circular and rougher than those processed by the ball mill.

---

**Keywords:** *HPGR, ball mill, particle size, particle shape, image analysis, SEM*

### **Introduction**

Particle size and shape are important parameters that can significantly affect mineral processing plants and pelletizing plant performances (Brozek and Surowiak, 2007). For example, using finer particles (with a certain size) in magnetic separation could improve the iron grade. The shape of crushed ore affects the product particle size in a ball mill grinding circuit. It has also been proposed that green pellet quality is directly related to the amount of fine particles in a pelletizing plant (Dwarapudi et al., 2008; Umadevi et al., 2008; Gul et al, 2014; Van der Meer, 2015). Particle size distribution and specific surface area (SSA) are also key factors that can control the quality of pellets. It is generally agreed that concentrates with Blaine specific surface areas higher than  $1800 \text{ cm}^2 \text{ g}^{-1}$  would result in pellets with superior quality (Meyer, 1980). Most iron ore processing plants produce concentrates with Blaine specific surface

areas of 500–1600 cm<sup>2</sup> g<sup>-1</sup>. The concentrate must therefore be re-ground in order to prepare suitable pellet feed.

High pressure grinding roll (HPGR) and ball mill are the most widely used machinery to increase Blaine specific surface areas of pellet feeds. Some pelletizing plants which use HPGR for regrinding are CVRD/Brazil, WISCO mineral/China, and Ardakan/Iran. In ball milling, particle size reduction occurs by impact and attrition breakage. It is established in ball milling, the particle size distribution curve of the product is generally parallel to the feed size (Bond, 1961). In HPGR, size reduction is attributed to compression and inter-particle abrasion breakage. Given the different force mechanisms used to reduce particle size in these two methods, it is expected that the shape of particles will be different (Pourghahramani and Forssberg, 2005). It is indicated that the shape of particles ground by HPGR would be more angular as compared to the ball mill product (Bleifuss, 1997). The particle size and shape of the pellet feed need to be characterized to learn how size and shape parameters affect pellet properties. The available literature regarding a comparison between ball mill and HPGR regrinding is limited.

Numerous techniques and devices have been developed and deployed for a particle size distribution analysis. These include sieve, image (IA) analyses and laser diffraction (Tasdemir et al, 2011; Arvaniti et al., 2014; Ilic et al., 2015). The sieve analysis is the most widely used method in mineral laboratories, but has limitations for the ultra-fine particles. The laser diffraction method is employed to study small particles (Ulusoy and Igathinathane, 2014). The image analysis can be an accurate method providing accurate information if applying appropriately (Boschetto and Giordano, 2012; Ilic et al., 2015).

Brunauer-Emmett-Teller (BET) and Blaine methods are established approaches for determining specific surface areas (SSA) of powder materials (Arvaniti et al., 2014). In the BET method, an inert gas, such as either nitrogen or argon, is physically adsorbed by the material surface. The entire surface area may thus be determined by measuring the amount of the adsorbed gas. However, this technique is time consuming and requires detailed sample preparation (Odler, 2003). The Blaine specific surface area of a powder is determined by measuring the permeability of air through a compact layer of sample. This method assumes a packed bed with a porosity of 50%, consisting of mono-sized spherical particles.

For the purpose of this study, five samples with Blaine specific surface areas of 1800–2200 cm<sup>2</sup> g<sup>-1</sup> were prepared by the ball mill and HPGR. The particle size distribution was carried out by three techniques. The specific surface area of each sample was measured by BET (SSA<sub>BET</sub>) and Blaine (SSA<sub>Blaine</sub>) methods. To characterize the shape of particles, three shape factors were obtained using a SEM micrograph and processed for the image analysis.

## Materials and methods

### Sample preparation

The iron ore concentrate was obtained from Gol-E-Gohar line 5 plant, South East of Iran. The concentrate was taken from the final belt filter with moisture of 9.4% wt. The concentrate was then completely dried in the oven. A 80% passing size ( $P_{80}$ ) and Blaine specific surface area of the concentrate were measured to be 133  $\mu\text{m}$  and 937  $\text{cm}^2\text{g}^{-1}$ , respectively. The chemical and sieve analyses of the concentrate are presented in Table 1 and Fig. 1.

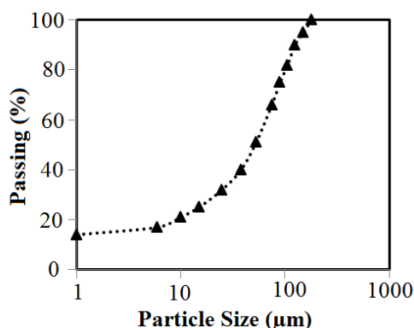


Fig. 1. Particle size distribution analysis of iron ore concentrate

Table 1. Chemical analysis of iron ore concentrate

Sample	Fe <sub>tot</sub>	FeO	S	P	MgO	CaO	Al <sub>2</sub> O <sub>3</sub>	SiO <sub>2</sub>	LOI*
Pellet feed (%wt)	69.85	26.75	0.13	0.05	0.41	0.18	0.25	1.19	2.58

\* Loss-on-ignition

Table 2. Ball mill process parameters for five ground samples with ball load  $J = 0.50$ , particle filling  $U = 0.53$ , mill speed  $N_c = 71\%$  and mill factor  $F_c = 0.69$

Test No.	Ball charge (% vol)	Grinding time (min)	SSA <sub>Blaine</sub> ( $\text{cm}^2\text{g}^{-1}$ )	$P_{80}$ ( $\mu\text{m}$ )
1	28.2	28.65	1800	42.6
2	28.2	32.65	1900	40.4
3	28.2	37.17	2000	38.3
4	29.6	37.82	2100	36.1
5	30.9	39.16	2200	34.1

Milling was carried out in a laboratory ball mill 312×284 mm (diameter × length). The ball distribution was fixed at equal volume fraction of 15 and 23 mm balls. The mill speed was set on  $N_c=71\%$ . The concentrate was charged to the mill and rotated for a specific time, and then discharged. Five samples with different Blaine specific

surface areas were prepared (Table 2). The theoretical  $SSA_{\text{Blaine}}$  is provided in Table 2 based on the previous research (Abazarpoor and Halali, 2016).

Grinding was performed in a pilot high pressure grinding rolls (HPGR), with the roll size  $0.25 \times 1$  m (length  $\times$  diameter). The feed was homogenized in a drum. The moisture content of samples was adjusted to 6.5 % wt in a horizontal mixer. In order to provide concentrate with  $SSA_{\text{Blaine}}$  between 1800–2200  $\text{cm}^2 \text{g}^{-1}$ , all the samples had to be preliminary ground in HPGR (Table 3).

Table 3. Primary grinding of iron ore concentrate by HPGR

Specification	Feed moisture (% wt)	Specific force ( $\text{N mm}^{-2}$ )	Roller speed (m $\text{s}^{-1}$ )	$SSA_{\text{Blaine}}$ ( $\text{cm}^2 \text{gr}^{-1}$ )	$P_{80}$ ( $\mu\text{m}$ )
Quantity	6.5	3.5	0.55	1540	62

The samples were subsequently ground in HPGR to the target  $SSA_{\text{Blaine}}$  of 1800–2200  $\text{cm}^2/\text{g}$ . It was essential to obtain Blaine numbers as close to ball mill samples as possible for a valid comparison. Table 4 represents data under grinding conditions.

Table 4. HPGR process parameters for five ground samples

Test No.	Feed moisture (% wt)	Specific force ( $\text{N mm}^{-2}$ )	Roller speed ( $\text{m s}^{-1}$ )	$SSA_{\text{Blaine}}$ ( $\text{cm}^2 \text{g}^{-1}$ )	$P_{80}$ ( $\mu\text{m}$ )
6	6.33	3	0.6	1800	41.8
7	6.14	3.41	0.56	1900	39.9
8	6.52	4.05	0.56	2000	37.9
9	6.51	4.43	0.52	2100	36.1
10	6.19	4.8	0.5	2200	34.3

## Particle size distribution

### Sieve and cyclosizer analysis

A wet screening analysis was performed in order to calculate the size distribution for each sample. A combination of Jones and rotary riffle was used to prepare representative sample. A 100 g of riffled sample was placed on the upper screen and water was passed with the flow rate of  $1 \text{ dm}^3/\text{min}$  and collected in a plastic container. A cyclosizer was used for size classification in the 6–45  $\mu\text{m}$  range.

### Laser analysis

The particle size distribution was performed with a Fritsch Analysette 22, capable for analysing particles between 0.08–1000  $\mu\text{m}$ . The sample was immersed in de-ionized water, and then de-agglomerated in an ultrasonic bath. Parameters were fixed at stirring speed of 1800 rpm, measurement time of 6.5 min and pulp concentration of 0.9 % wt.

### Particle shape and size by SEM using image analysis

SEM with secondary electron images was used to determine the particle size and shape using image analysis. It is a prime requirement of the image analysis (IA) method that measurements shall be made on isolated particles. There should be as few particles as possible touching each other (ISO13322-1, 2014). In order to reduce particles touching problem, the selected sample was first completely dispersed in ethanol using an ultrasound bath (Vaziri Hassas et al., 2016), and then filtered to dry. However, there was still a small error of 2D projection due to ultra-fines adherence to coarse particles.

Part of the sample was coated with a thin layer of gold in order to get the sample sufficiently conductive. The images were taken at 1000-3000 magnifications. A number of images were generated in different zones of the sample. ImageJ 1.46n software was employed to provide different shape descriptors. This software makes the assumption that binary images consist of white background and black objects (Ferreira and Rasband, 2011; Ilic et al., 2014). This process was applied for images to provide precise size and shape measurements: (a) size calibration, (b) normalized contrast enhancement, (c) background noise reduction, (d) threshold to extract particles from background, (e) 'watershed' and 'exclude on edge' techniques to minimize particles touching effect.

As can be seen from Fig. 2, there is number of fine particles adhered on the coarse particles (Fig. 2a) which may change the general contour of the particle image (Fig. 2b). In such case, size and shape measurements were performed on the real image of particles without making silhouette of particles (Fig. 2c). The picture threshold was stopped and SEM pictures were used directly without make binary pictures (black and white). It enabled to correctly distinguish fine and coarse particles.

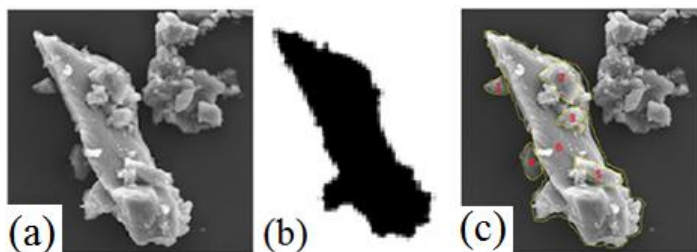


Fig. 2. Differentiating method for fine particle adherence to coarse one: (a) SEM micrograph, (b) Silhouette picture, (c) fine particle separation from coarse particles

In order to determine the particle size and shape using ImageJ software 3000-3100 particles were analysed. According to the standard ISO13322-1, it was necessary to perform 3096 particles to achieve the low error value. A size distribution described by the number of particles required a smaller number of particles to be count than for distribution by the volume (ISO13322-1, 2014).

Figure 3 lists the measured shape descriptors, their definitions and pictorial examples. In order to indicate the variability of size and shape factors arithmetic average alongside standard deviation is reported (Vaziri Hassas et al., 2016).

An equivalent circle diameter (ECD) was measured for the particle size distribution curve. Using SEM, the area measurement from the image was used to determine the diameter of a circle with equivalent area to the image. The diameter of this circle was then considered as ECD of the particle. Circularity was computed from the projected area ( $A_p$ ) and was equal to 1.0 for a perfect circle and less than 1.0 for elongated shaped particles. The roughness had values either equal or higher than 1.0 and was calculated by dividing area of the smallest circumscribed circle to area of projected particle. A smooth shape has a roughness of 1 and irregular particles tend to have higher roughness values. The aspect ratio is always either equal or greater than 1.0. A symmetrical shape in all axes, such as a sphere has aspect ratio of 1, while an infinite elongated particle has a higher aspect ratio (Boschetto and Giordano, 2012; Ilic et al., 2015).

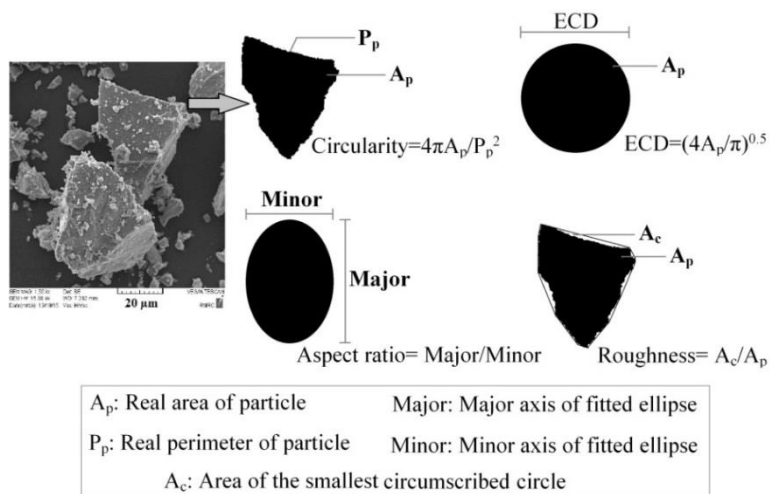


Fig. 3. Shape and size factors equation and definition (Ferreira and Rasband, 2011)

### Specific surface area determination

In this Blaine test, the air permeability of a bed of fine particles was assumed to be inversely proportional to the fineness of the particles (ASTM C-204, 2011). Therefore, the time needed for air to pass through the particles bed gave an indication of surface area.

In the BET technique, an adsorption isotherm was measured by plotting the volume of gas adsorbed versus the pressure ( $P$ ) of  $N_2$  gas. Calculation of the specific surface area was based on the extension of the Langmuir theory to a multi-molecular layer adsorption.

## Results and discussion

### Particle size distribution

Particle size distributions determined by sieve, laser and image techniques are shown in Fig. 4 for the coarsest and finest samples of ball mill and HPGR. Sieve and cyclosizer analyses are unable to provide the distribution of particles smaller than 6  $\mu\text{m}$ , so the result of the IA method was considered for this size range. In most cases, the laser diagram indicates a greater fraction passing for particles  $<10 \mu\text{m}$  than the IA curve. For particles in the size range of 10-80  $\mu\text{m}$  the laser curve is above the IA curve. For particles larger than 80  $\mu\text{m}$  the diagram obtained by IA is above that obtained by laser.

The main reasons for the discrepancy in results between laser and the other two methods may be attributed to (Arvaniti et al., 2014; Ilic et al., 2015): (a) effect of ultrasound application, (b) insufficient dispersion of fine particles, (c) fine particles adhering to the coarser particles, (d) nature of techniques, (e) low concentrations of particles in the laser measurement, (f) materials nature in the laser measurements.

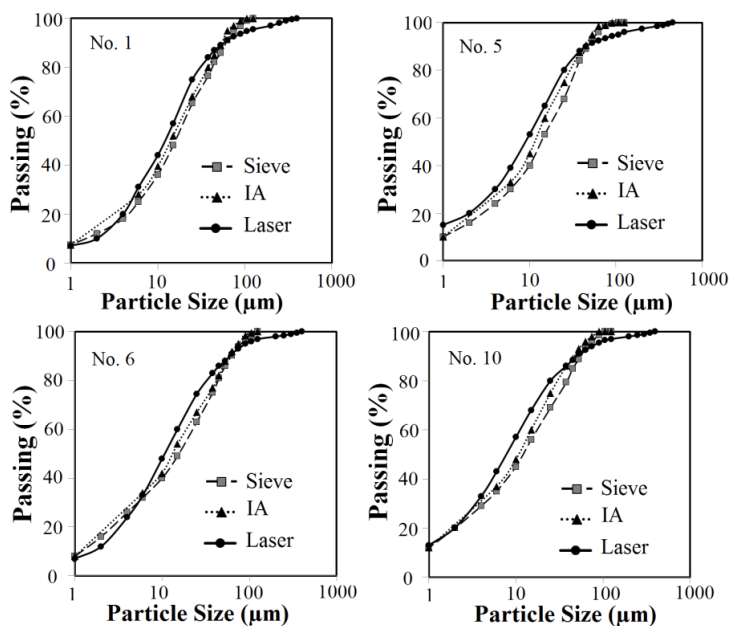


Fig. 4. Particle size distribution obtained from laser, IA and sieve methods for ball mill (No. 1, 5 samples) and HPGR (No. 6, 10 samples)

It is worth mentioning that the sieve analysis for the current study was close to that obtained by IA. In order to show this claim the deviation of laser and sieve results from the IA method using  $\%< 10 \mu\text{m}$  and  $\%< 80 \mu\text{m}$  are shown in Table 5. The average deviation of  $\%< 10 \mu\text{m}$  for laser and sieve was 6.4 and 2.7  $\mu\text{m}$ , respectively.

Also, the average distance of %< 80  $\mu\text{m}$  for laser and sieve was 5.7 and 1.8  $\mu\text{m}$ , respectively. Therefore, the deviation between the sieve and image was less than the laser analysis.

Table 5. Deviation of laser and sieve analysis results from IA method using %< 10  $\mu\text{m}$  and %< 80  $\mu\text{m}$  quantities

No.	%< 10 $\mu\text{m}$			%< 80 $\mu\text{m}$			%< 10 $\mu\text{m}$		%< 80 $\mu\text{m}$	
	IA	Sieve	Laser	IA	Sieve	Laser	IA-sieve	IA-laser	IA-sieve	IA-laser
1	39	36	44	98	95	91	3	5	3	7
2	40	38	42	98	95	88	2	2	3	10
3	41	38	55	99	98	92	3	14	1	7
4	44	40	44	100	99	92	4	0	1	8
5	46	40	54	100	99	95	6	8	1	5
6	41	39	48	95	94	93	2	7	1	2
7	44	43	52	97	95	94	1	8	2	3
8	45	43	51	98	97	93	2	6	1	5
9	46	45	53	99	96	94	1	7	3	5
10	49	46	56	99	97	94	3	7	2	5

For samples ground by a ball mill, it was observed that the fraction of particles <10  $\mu\text{m}$  increased from 39 to 46% as the Blaine number increased from 1800 to 2200  $\text{cm}^2\text{g}^{-1}$ . For HPGR samples, corresponding data were 41 and 49% respectively. It was evident that for samples ground by HPGR, the fraction of fine particles was higher than that of those ground in the ball mill (samples with the equal Blaine numbers). For pellet feed preparation, HPGR was therefore more appropriate when finer particles and higher real surface area were desired. This observation is in line with previous studies (Abouzeid and Fuerstenau, 2009). In HPGR grinding, size reduction took place in a particle bed, and disintegration of ore particles took place through inter-particle crushing in the particle bed between the rolls. In contrast, ball mills relied on single particle breakage for their size reduction, as a contact crushing between balls. Hence, a larger fraction of fine particles was inherent in HPGR (van der Meer, 2015).

### Specific surface area analysis

Two methods were employed for precise measurement of specific surface area of each sample. Apart from the nature of the particles, the Blaine technique was significantly affected by the compaction level of the bed and shape of particles. The Blaine method is therefore considered a relative process (Arvaniti et al., 2014). The BET technique, on the other hand is able to measure closer to the true surface area of particles. This technique assumes that a monolayer of an inert gas is absorbed onto the surface of particles. Unlike the Blaine method, cracks and porosity within the particles are therefore taken into account in the BET technique (Zielinski and Kettle, 2013).



The values of specific surface area of the particles determined by the Blaine and BET methods are presented in Fig. 5. All the results indicate larger  $SSA_{BET}$ . The reason for this observation as described before lies on the nature of these two methods. The BET method measures closer to the true surface area of particles including roughness, and cracks and is therefore more accurate (Arvaniti et al., 2014). Also, the fact that particles are not equally sized spheres with a packing density of 50% (Blaine assumption), may be a key reason.

It can be observed that samples ground by HPGR had higher  $SSA_{BET}$  values than those ground by the ball mill. The reason may be attributed to the superior effect of micro/macro cracks within particles, higher fine particles and HPGR increased the Blaine specific surface area as a result of compression grinding and abrasion of the particle surfaces (van der Meer, 2015) compared to ball mill grinding. Micro cracking is the phenomenon whereby internal fracturing of particles occurs due to the extreme pressures exerted by the rolls in the compression zone (Morley, 2010).

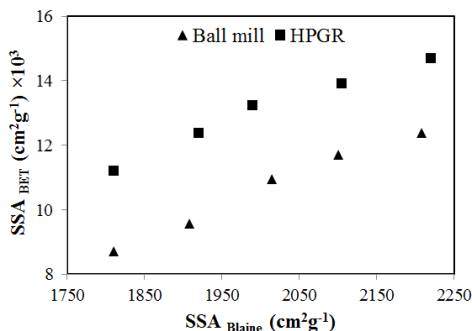


Fig. 5. Specific surface area of particles by the Blaine and BET methods for ball mill and HPGR

### Particle shape studies

The iron ore particles are non-isometric with irregular shapes, as can be seen in the SEM micrographs in Fig. 6, so several shape factors are required in order to fully characterize them. However, there is still a small limitation for size and shape measurements owing to particles agglomeration.

The mode of breakage, whether a single particle or inter-particle, is suggested to play an important role in generating particles with different shapes. In HPGR grinding, the surface discontinuities tend to shrink to smaller diameters by having sharper edges, corners and more irregular shapes due to the compressive nature of HPGR grinding (Zhu et al., 2004; Van der Meer, 2015).

As illustrated in Fig. 7, particles ground in the ball mill had higher circularity (0.795-0.850) in comparison to HPGR products (0.698-0.671). During ball mill grinding, circularity increased, whereas in HPGR decreased with the Blaine number. This observation was due to different breakage mechanisms in these two systems. In

the ball mill, breakage was mainly due to impact and attrition. In HPGR, compaction and inter particle abrasion were chiefly responsible for breakage.

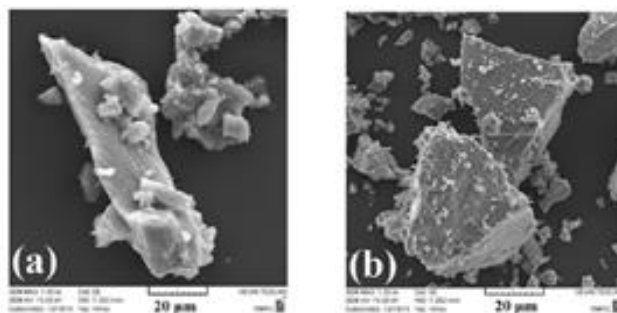


Fig. 6. SEM micrograph of samples after (a) HPGR and (b) ball mill

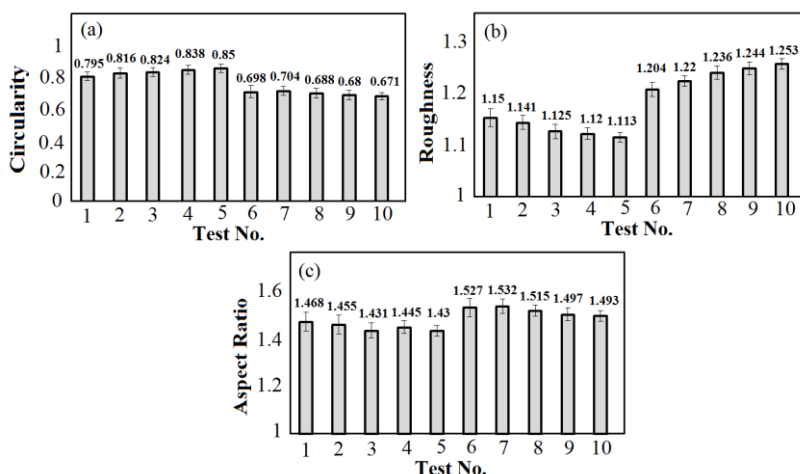


Fig. 7. Shape factors including (a) circularity, (b) roughness and (c) aspect ratio for ball mill (No. 1–5) and HPGR (No. 6–10) (error bars show standard deviation)

The roughness factor decreased for ball mill particles and contrarily increased for HPGR particles when the Blaine number increased. This fact indicates that as particles were ground more in the ball mill, their surface tended to be less rough, while using HPGR provided rougher and more angular surfaces. Overall, the particles ground in the HPGR were rougher compared to those ground in the ball mill which was considered a result of the different breakage mechanisms of each grinding method. It was evidence that size reduction by pressure (HPGR) resulted in rough particles, whereas size reduction by attrition (ball mill) produced rounded particles.

Figure 7 indicates that the aspect ratio was reduced in both the ball mill and HPGR as the Blaine number increased. This is an indication that elongated particles tended to break as grinding proceeded. It is also evident that samples ground in HPGR had

higher aspect ratios than those ground in the ball mill (Bleifuss, 1997). This is considered to be a result of the inter-particle breakage mechanism occurring in HPGR.

A statistical analysis (Fig. 7) on circularity, roughness and aspect ratio descriptors showed a maximum of 5% deviation for each of these descriptors.

## Conclusions

From the grinding results using the ball mill and HPGR the following conclusions can be drawn.

- For equal Blaine numbers, the amount of fine particles ( $\% < 10 \mu\text{m}$ ) was higher for HPGR. This was related to differences in the breakage mechanism of the ball mill and HPGR.
- In all samples  $SSA_{\text{BET}}$  was higher than  $SSA_{\text{Blaine}}$ , because the BET technique measured closer to the true surface area of particles including porosity, cracks and roughness of particles.
- For equal numbers of  $SSA_{\text{Blaine}}$ ,  $SSA_{\text{BET}}$  after grinding by HPGR was higher than the ball mill product due to the superior effect of micro/macro cracks within particles, higher fine particles, creation of new surfaces and porosity in the particles compared to ball mill grinding.
- It was demonstrated that HPGR produced particles that were more elongated, less circular and rougher than those processed by the ball mill.

## Acknowledgements

The authors would like to express their appreciation to FSTCO laboratory and specially Mr. Saghaeian and Mr. Hejazi for their comprehensive support.

## References

- ABAZARPOOR, A., HALALI, M., 2016, *Optimization of Particle Size and Specific Surface Area of Pellet Feed in Dry Ball Mill using Central Composite Design*, Indian Journal of Science and Technology, 44, 1-10.
- ABOUZEID, A.M., FUERSTENAU, D.W., 2009, *Grinding of mineral mixtures in high-pressure grinding rolls*, International Journal of Mineral Processing, 93, 59-65.
- ARVANITI, E. C., JUENGER, M. C. G., BERNAL, S. A., DUCHESNE, J., COURARD, L., LEROY, S., PROVIS, J. L., KLEMM, A., BELIE, N. D., 2014, *Determination of particle size, surface area, and shape of supplementary materials by different techniques*, Materials and Structures, 48, 3687-3701.
- ASTM C204-11, 2011. *Standard test methods for fineness of hydraulic cement by air-permeability apparatus*.
- BLEIFUSS, R., 1997. *MBR Pellet Feed Investigations*, Internal Reporting of KHD & Coleraine Minerals Research Laboratory.
- BOND, F.C., 1961, *Crushing and grinding calculations Part I and II*, British Chemical Engineering, 6, 378-385.
- BOSCHETTO, A., GIORDANO, V., 2012, *Powder sampling and characterization by digital image analysis*, Measurement, 45, 1023-1038.

- BROZEK, M., SUROWIAK, A., 2007, *Effect of particle shape on jig separation efficiency*, Physicochemical Problems of Mineral Processing, 41, 397-413.
- DWARAPUDI, S., DEVI, T. U., MOHAN RAO, S., RANJAN, M., 2008, *Influence of pellet size on quality and microstructure of iron ore pellets*, The Iron and Steel Institute of Japan International, 48, 768-776.
- GUL, A., SIRKECI, A.A., BOYLU, F., GULDAN, G., BURAT, F., 2014, *Improvement of mechanical strength of iron ore pellets using raw and activated bentonites as binders*, Physicochemical Problems of Mineral Processing, 51, 23-36.
- FERREIRA, T., Rasband, W., 2011. The ImageJ user guide 1.44.
- ILIC, M., BUDAK, I., KOSEC, B., NAGODE, A., HODOLIČ, J., 2014, *The analysis of particles emission during the process of grinding of steel en 90mnv8*, Metalurgija, 53, 189-192.
- ILIC, M., BUDAK, I., VUCINIC, M., NAGODE, A., KOZMIDIS-LUBURIC, U., HODOLIC, J., PUŠKAR, T., 2015, *Size and shape particle analysis by applying image analysis and laser diffraction – Inhalable dust in a dental laboratory*, Measurement, 66, 109-117.
- ISO 13322-1, 2014. *Particle size analysis by Image analysis methods, Part 1: Static image analysis methods*.
- MAZZOLI, A., FAVONI, O., 2012, *Particle size, size distribution and morphological evaluation of airborne dust particles of diverse woods by scanning electron microscopy and image processing program*, Powder Technology, 225, 65-71.
- MEYER, K., 1980. *Pelletizing of Iron Ore*, Springer Berlin Heidelberg.
- MORLEY, C., 2010, *HPGR-FAQ*, The Journal of The Southern African Institute of Mining and Metallurgy, 110, 107-115.
- ODLER, I., 2003, *The BET-specific surface area of hydrated Portland cement and related materials*, Cement and Concrete Research, 33, 2049-2056.
- POURGHAMRANI, P., FORSSBERG, E., 2005, *Review of applied particle shape descriptors and produced particle shapes in grinding environments. part ii: the influence of comminution on the particle shape*, Mineral Processing & Extractive Metallurgy Review, 26, 167-186.
- TASDEMIR, A., OZDAG, H., ONAL, G., 2011, *Image analysis of narrow size fractions obtained by sieve analysis - an evaluation by log-normal distribution and shape factors*, Physicochemical Problems of Mineral Processing, 46, 95-106.
- ULUSOY, U., IGATHINATHANE, C., 2014, *Dynamic image based shape analysis of hard and lignite coal particles ground by laboratory ball and gyro mills*, Fuel Processing Technology, 126, 350-358.
- UMADEVI, T., SAMPATH KUMAR, M.G., KUMAR, S., GURURAJ PRASAD, C.S., RANJAN, M., 2008, *Influence of raw material particle size on quality of pellets*, Ironmaking & Steelmaking, 35, 327-337.
- VAN DER MEER, F.P., 2015, *Pellet feed grinding by HPGR*, Minerals Engineering, 73, 21-30.
- VAZIRI HASSAS, B., CALISKAN, H., GUVEN, O., KARAKAS, F., CINAR, M., CELIK, M.S., 2016, *Effect of roughness and shape factor on flotation characteristics of glass beads*, Colloids and Surfaces A: Physicochemical and Engineering Aspects, 492, 88-99.
- ZHU, D., PAN, J., QIU, G., CLOUT, J., WANG, C., GUO, Y., HU, C., 2004. *Mechano-chemical activation of magnetite concentrate for improving its pellet-ability by high pressure roll grinding*. ISIJ International. 44, 310-315.
- ZIELINSKI, J.M., KETTLE, L., 2013. *Physical Characterization: Surface Area and Porosity*, White paper, Intertek Chemicals and Pharmaceuticals.